ACCURACY EVALUATION OF STRUCTURE FROM MOTION THERMAL MOSAICING IN THE CENTER OF TOKYO

Atik Nurwanda[1], Tsuyoshi Honjo[1]*, Nobumitsu Tsunematsu[2], and Hitoshi Yokoyama[3]
[1]Graduate School of Horticulture, Chiba University, 648, Matsudo, Matsudo-shi, Chiba, Japan.
[2]Tokyo Metropolitan Research Institute for Environmental Protection, Tokyo Environmental Public Service Corporation, 1-7-5 Shinsuna, Koto-ku, Tokyo, Japan.
[3]National Research Institute for Earth Science and Disaster Resilience, 3-1 Tennodai, Tsukuba-shi, Ibaraki, Japan.
*e-mail: honjo@faculty.chiba-u.jp

Received: 11 December 2017; Revised: 12 October 2018; Approved: 6 December 2018

Abstract. In the airborne and high-resolution measurement of Land Surface Temperature (LST) over large area, capturing and synthesizing of many images are necessary. In the conventional method, the process of georeferencing a large number of LST images is necessary to make one large image. Structure from Motion (SfM) technique was applied to automized the georeferencing process. We called it "SfM Thermal Mosaicing". The objective of this study is to evaluate the accuracy of SfM thermal mosaicing in making an orthogonal LST image. By using airborne thermal images in the center of Tokyo, the LST image with the 2m resolution was created by using SfM thermal mosaicing. Its accuracy was then analyzed. The result showed that in the whole examined area, the mean error distance was 4.22m and in the small parts of the examined area, the mean the error distance was about 2m. Considering the image resolution, the error was minimal indicating good performance of the SfM thermal mosaicing. Another advantage of SfM thermal mosaicing is that it can make precise orthogonal LST image. With the progress of UAV and thermal cameras, the proposed method will be a powerful tool for the environmental researches on the LST.

Keywords: *accuracy evaluation, the center of Tokyo, georeferencing, structure from motion, land surface temperature, orthogonal.*

1 INTRODUCTION

Land surface temperature (LST) is widely used in urban heat island (UHI) studies and other environmental researches. There have many studies which analyzed the LST of satellite images (Chen *et al.* 2014; Connors *et al.* 2013; Dousset and Gourmelon 2013; Estoque *et al.* 2017; Streutker 2002; Weng *et al.* 2004). The resolution of commonly used satellite-derived LST are 100m (Landsat 8 TIRS), 60m (Landsat ETM), 90m (Terra ASTER), Landsat TM (120m), 1km (MODIS), 1.1km (NOAA), 1km (ENVISAT), and 3km (Meteosat) (Darlington *et al.* 2017). Airborne measurement of high-resolution LST is preferable to analyze the detail of urban environment because the size of roads and buildings are mostly less than 10m.

In the airborne and high-resolution measurement of LST over a large area, capturing and synthesizing of many images are necessary because the airborne thermal camera can only take the LST of a small area. In the conventional method, the process of georeferencing and mosaicing small LST images is necessary to make one large image. The manual positioning of many ground control points (GCPs) should be done in georeferencing of each LST images.

http://dx.doi.org/10.30536/j.ijreses.2018.v15.a2856

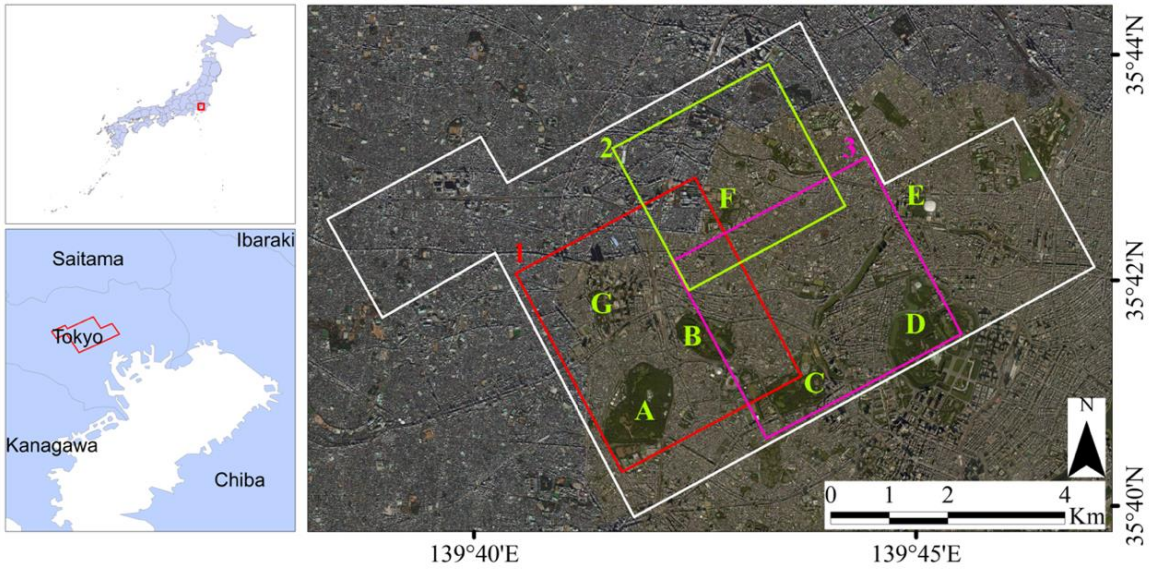

Figure 1-1: The area of interest in the center of Tokyo. The aerial photo on the map was taken on August 19th, 2014. The white border is a large area used for the analysis. The squares of 1, 2, and 3 are the small analyzed areas. (A. Yoyogi Park & Meiji Jingu Shrine, B. Shinjuku Goen National Garden, C. Akasaka Palace, D. Imperial Palace, E. Koishikawa Korakuen Garden, F. Korakuen Garden, and G. Shinjuku Chuo Park).

These processes require a lot of labor force and time if the images are in large quantities. Hence, this difficulty even influences the decision to make the measurement.

To solve this problem, Honjo *et al.* (2017) applied Structure from Motion (SfM) technique to the georeferencing and mosaicing process and named the process as "SfM thermal mosaicing". Formally, thermal images were not used in the process of SfM because of its low resolution and low contrast, but in SfM thermal mosaicing only thermal images were used to make an orthogonal LST image. The method effectively reduces the labor of obtaining GCPs in georeferencing. Honjo *et al.* (2017) also analyzed the relation between urban LST change and urban morphology. In the study, the LSTs of the two periods were overlaid, and the difference was well detected. But in the overlaid process, the pixel to pixel coincidence was impossible, and the detailed analysis of the accuracy of the technique was not made. The quantitative accuracy measurement is necessary for the further application of SfM thermal mosaicing to the LST analysis.

SfM has been used in many studies where 3D models were made from photographs (Colomina and Molina, 2014; Westoby *et al.* 2012), i.e., 3D mapping for surveying earthwork projects (Siebert and Teizer 2014), 3D mapping of vegetation spectral dynamics (Dandois and Ellis 2013), 3D reconstruction of sedimentary outcrops (Chesley *et al.* 2017), urban flood modelling (Meesuk *et al.* 2015), and topographic survey (James *et al.* 2017).

In this study, we evaluated the accuracy of LST image made by SfM thermal mosaicing process. By using airborne thermal images in the center of Tokyo, the LST image was made by using SfM thermal mosaicing, and its accuracy was measured. In the analysis of the accuracy, the LST image and Google Map image were overlaid, and the distances of the corresponding referenced points of both images are defined as an error distance. From the measurement of the error distances, we analyzed the accuracy of the method.

2 MATERIALS AND METHODOLOGY

2.1 Location and Data

The analyzed area is shown in Figure 1-1. It is the center area of Tokyo, including Shinjuku area and north area of Imperial Palace. The area is a typical urban area which includes high-rise buildings, low-rise buildings, and urban green areas (Imperial Palace, Shinjuku Gyoen National Garden, Yoyogi Park, Koishikawa Korakuen Garden, etc.). Airborne thermal images were used which were taken on August 19th, 2014 from the height of 600m above surface land.

2.2 SfM Thermal Mosaicing

The comparison of SfM thermal mosaicing and conventional method of manual georeferencing process are described in Figure 2-1. The original images are a small thermal image in the daytime and night-time. In SfM thermal mosaicing, we used 3065 daytime images and 3097 night-time images. Each image is 599x451 pixels (8bit and grayscale) with 2m resolution. From the original images, we made daytime and night-time LST image. In SfM thermal mosaicing process, Photoscan Pro (Agisoft) was used. After the SfM thermal mosaicing process, the image was georeferenced only once on the map.

In the conventional method of manual georeferencing process (Figure 2-1, B), detecting at least three GCPs were necessary for each image and detection of GCPs should be done for all original images. After georeferencing process, the mosaicing process was executed to make the LST image. The human error for each georeferencing process affects the accuracy of LST image. To compare the SfM thermal mosaicing and manual georeferencing, daytime and night-time images made by Skymap Inc. was used as examples of manual georeferencing images (Figure 2-1, B3).

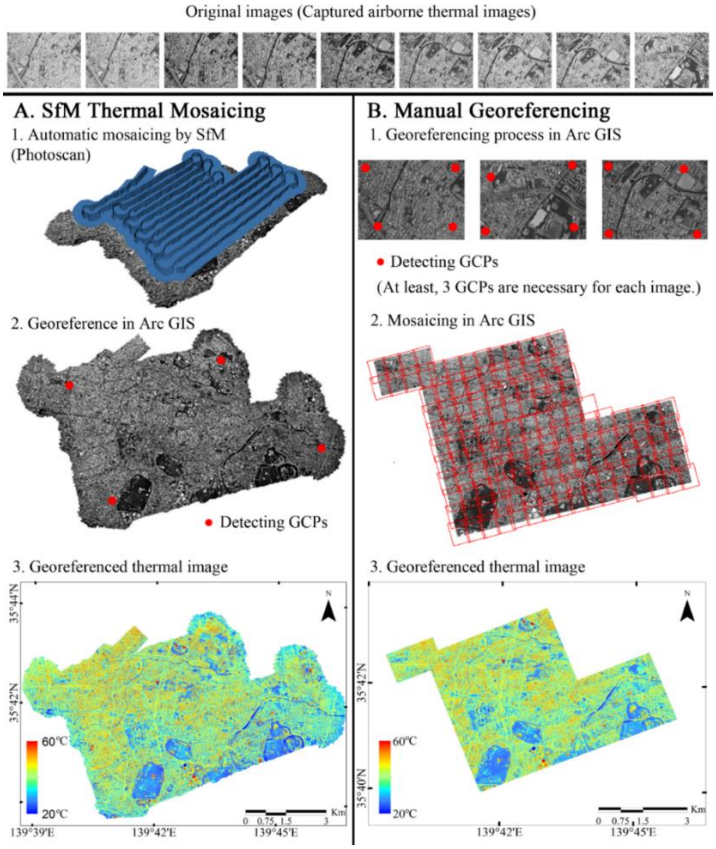

Figure 2-1: SfM thermal mosaicing and manual georeferencing

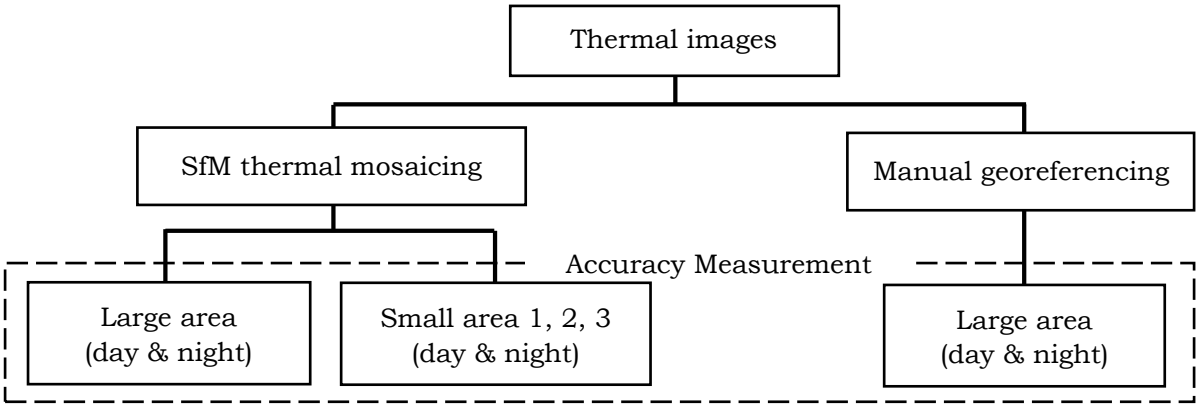

Figure 2-2: Flowchart of accuracy measurement

2.3 Accuracy Measurement

Flowchart of the accuracy assessment is shown in Figure 2-2. To measure the accuracy, we used SfM thermal mosaicing and manual georeferencing images of large area (whole analyzed area) both in daytime and night-time. We also analyzed small area (three small parts of the area shown as squares 1, 2 and 3 in Figure 1-1). In manual georeferencing, the only large area is analyzed because the error distance is relatively same either large and small areas. In the SfM thermal mosaicing, georeferencing process was - conducted once for large small areas, respectively. For accuracy evaluation, the accuracy of LST image was analyzed for large and small areas. The same procedure of accuracy analysis was conducted for a large area of manual georeferencing image.

Twenty sample points were selected at the point of the building edges, the cross-section center, and the corner of the bridges on each LST image in Figure 2-2 (a large area and three small areas in SfM thermal mosaicing, and a large area in manual georeferencing).

The accuracy measurement is illustrated in Figure 2-3. The red dot represents the reference point in Google Map which is the same place as the sample point of the overlaid LST image. The distance between the reference point and the sample point was defined as the error distance. The error distance (*ED*) is expressed by the following formula:

$$ED = \sqrt{(x1 - x2)^2 + (y1 - y2)^2} \qquad (2\text{-}1)$$

where, *(x1, y1)* is a reference point on the Google Map, *and (x2, y2)* is the sample point on the LST image. The error vector is also defined as $(x2 - x1, y2 - y1)$.

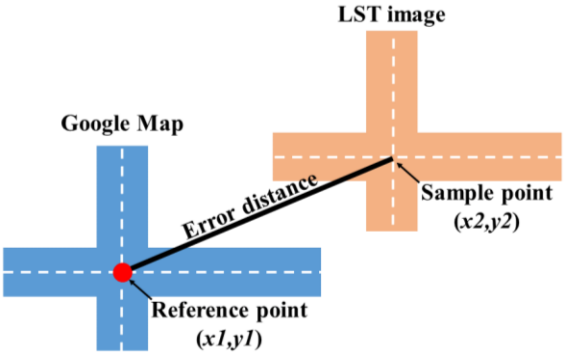

Figure 2-3: Diagram of measurement of error distance.

When the error distance value is low, it means the accuracy is high. The error distance measurement was conducted in Q-GIS which connected with Google Map. The error distance was adjusted as the mean x- and y-component of error distance become zero (0) as follows:

$$\sum(x1 - x2) = 0 \quad (2\text{-}2)$$

$$\sum(y1 - y2) = 0 \quad (2\text{-}3)$$

3 RESULTS AND DISCUSSION

3.1 Daytime and Night-time LST Image with SfM Thermal Mosaicing

The LST images of the daytime and night-time large area by SfM thermal mosaicing are shown in Figure 3-1. The process of making the LST image of the large area took about 45 hours with PC for (CPU: Intel Core i7-4790K, Memory: 12GB). The result showed that the standard deviation of daytime LST images is 16.52°C and night-time LST image is 8.87°C. The standard deviation of daytime LST image was wider than that of night-time LST image because LST value was higher in the daytime. The standard deviation was quite wide range either in the daytime and nighttime representing the variety of the objects of the urban surface, i.e., water surfaces, green areas, roads, and buildings.

Daytime LST image is more clear and has a clear contrast because the temperature difference in the daytime LST distribution is larger than that in the night-time LST distribution. In the daytime, hot areas were observed in the building, the cross-section of roads, square, etc. Meanwhile, cool areas were observed in urban trees, lawn area (grass), and water. Edges of these objects were well recognized with the resolution of the images. On the other hand, the standard deviation of night-time LST image is relatively narrow. It implies the recognition of the objects is slightly difficult in the night-time.

3.2 The Accuracy of SfM Thermal Mosaicing

The error vectors in automatic georeferencing with SfM thermal mosaicing are shown in Figure 3-1. The red dot represents the center of the reference point, and the black line is the error distance. The directions of errors are randomly distributed. The error distance of daytime and night-time thermal images are 4.22m and 4.65m, respectively (Figure 3-4). The error distance of daytime thermal image is a slightly better than night-time thermal image. One of the reasons is that the objects in night-time thermal images were more obscure in the SfM thermal mosaicing.

In Figure 3-2, the accuracy of the small areas (1, 2, & 3) is shown. Comparing Figure 3-1 and Figure 3-2, the error distance of the small areas area mostly shorter than the error distance of the large area both day and night. The error distance of small areas ranges from 1.80m to 2.76m, while large area range from 4.22m to 5.18m (Figure 3-4).

3.3 The Accuracy of Manual Georeferencing

The error vector of manual georeferencing of the large area is shown in Figure 3-3. The error vector is randomly distributed. As the result of the SfM thermal mosaicing in Figure 3-1, the error distance of manual georeferencing in daytime thermal image is slightly better than night-time thermal image.

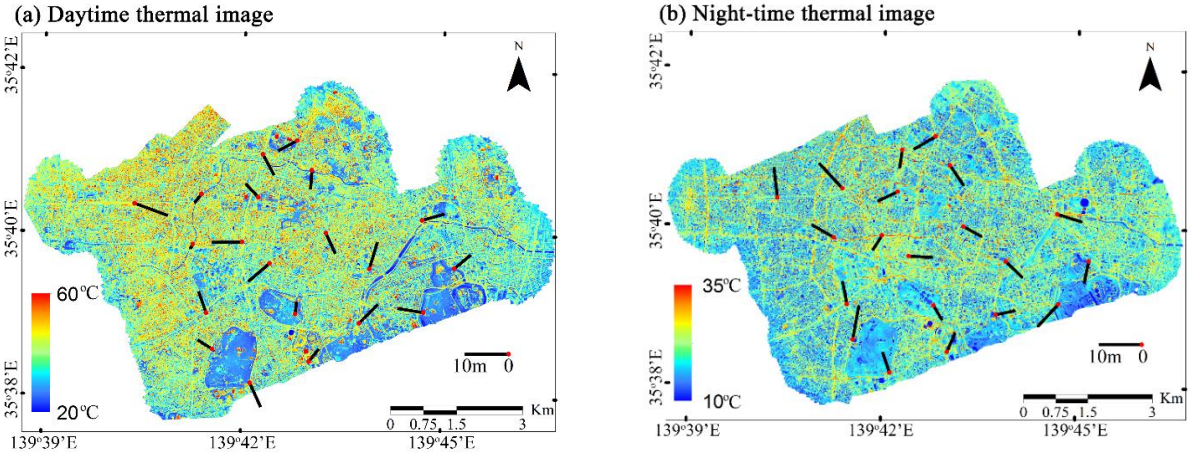

Figure 3-1: Images of error vector in SfM thermal mosaicing (large area).

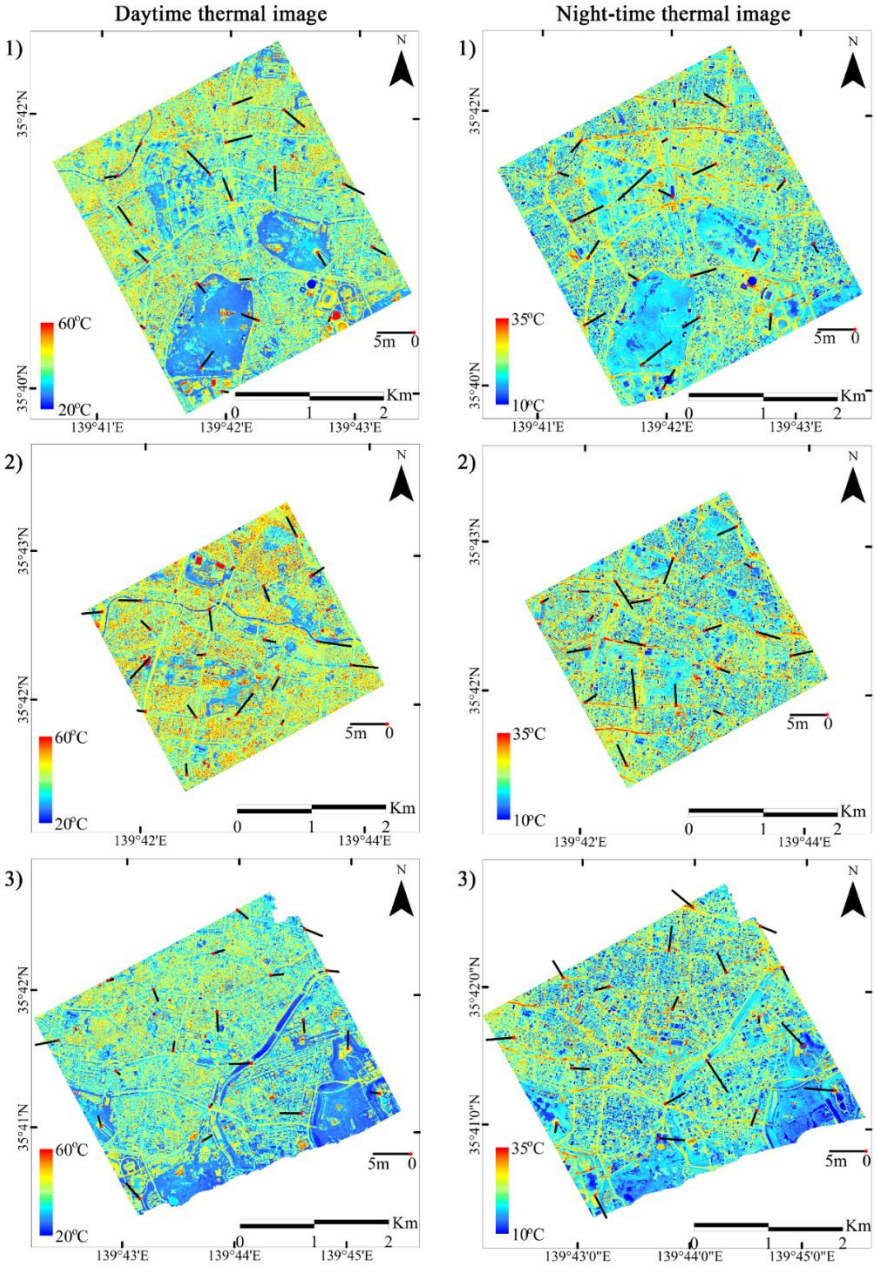

Figure 3-2: Images of error vector in SfM thermal mosaicing (small area).

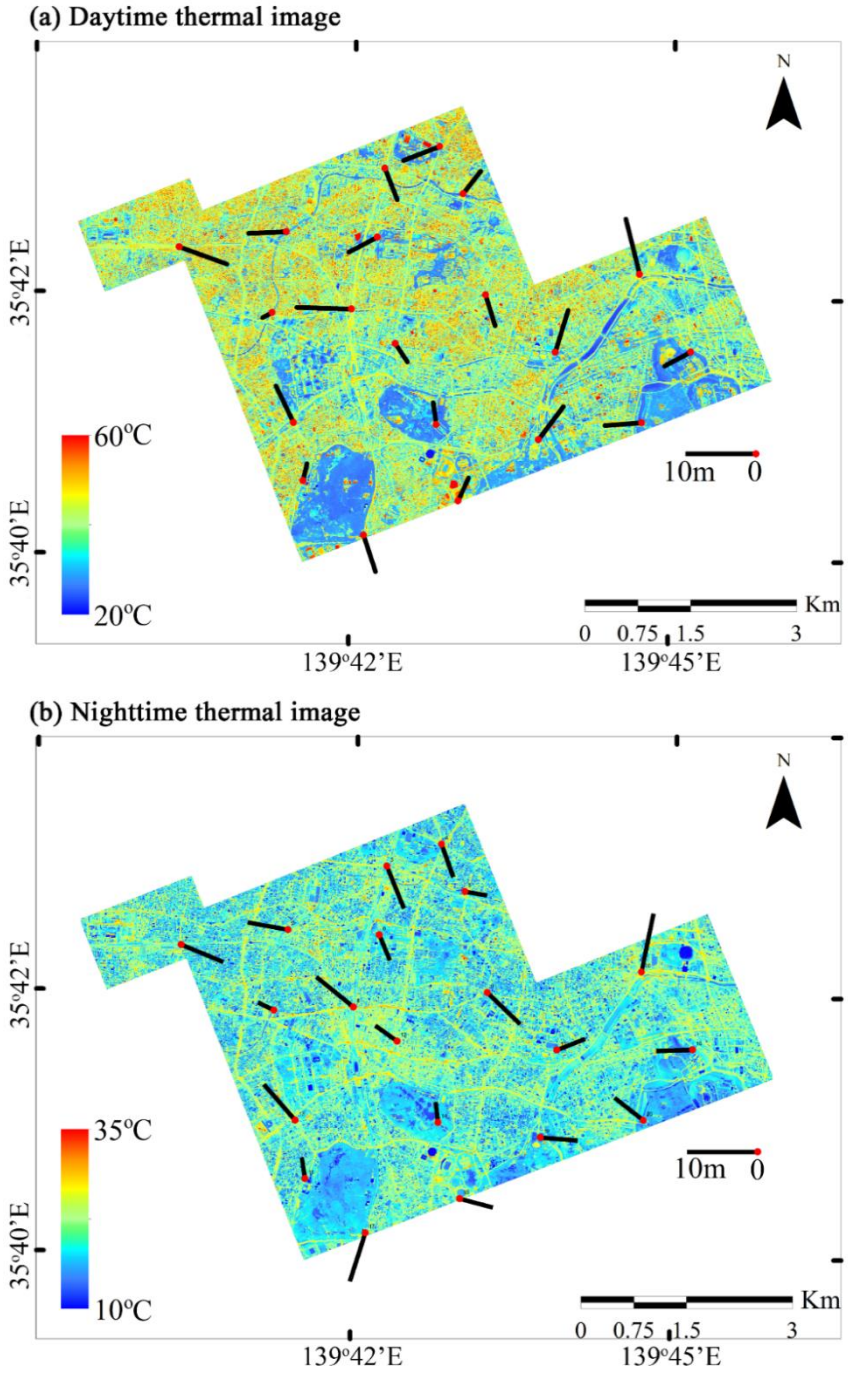

Figure 3-3: Images of error vector in manual georeferencing.

3.4 Accuracy Comparison

The error distance in Figure 3-1, 3-2, and 3-3 are summarized in Figure 3-4. The accuracy of LST image made by SfM thermal mosaicing in a large area is 4.22m (daytime) and 4.65m (night-time). While in small areas, their accuracy is about 2m. Considering the resolution of the image is 2m, the accuracy is nearly the best.

The error distances of manual geo-referencing in the large area are 5.05m (daytime) and 5.18m (night-time). The error distance of SfM thermal mosaicing is almost the same as that of manual georeferencing.

3.5 The Advantage of SfM Thermal Mosaicing

In SfM thermal mosaicing process in this study, no GCPs are used. But, even though there is no GCPs, we found that SfM thermal mosaicing was accurate to make the LST images (Figure 3-4).

In the case of manual georeferencing, it is difficult to use all the overlapped images because it is convenient to use fewer and less overlapped images to reduce the time for manual georeferencing process. In the SfM thermal mosaicing, overlapping of the images has a good effect in making an orthographic image.

3.6 Image Quality of Automatic Georeferencing Thermal Image

Images of SfM thermal mosaicing and manual georeferencing are compared in Figure 3-5. In the case of manual georeferencing, many sides (walls) of high

buildings remain as the dark blue shadow in Figure 3-5b. While there is no reducing process of side building in manual georeferencing, the SfM thermal mosaicing can reduce the side of buildings, and the image becomes orthogonal as shown in Figure 3-5a. In the process of detection of corresponding points by SfM thermal mosaicing, the points in the original images are calculated as an orthogonal point cloud.

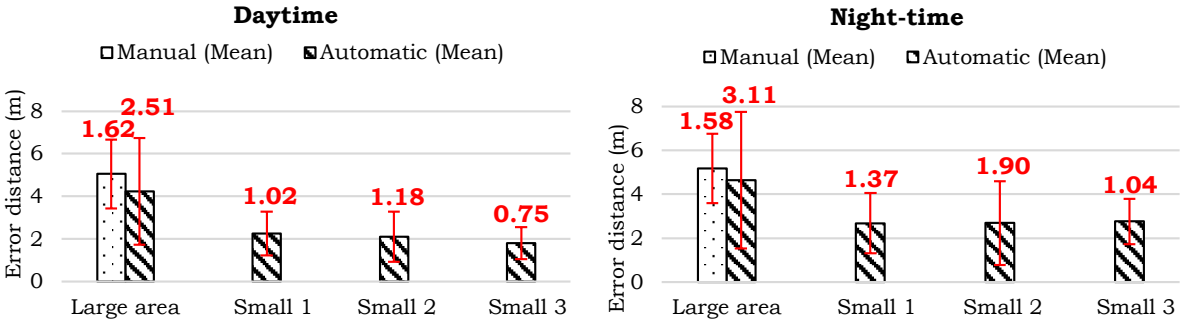

Figure 3-4: Mean and standard deviation of error distance.

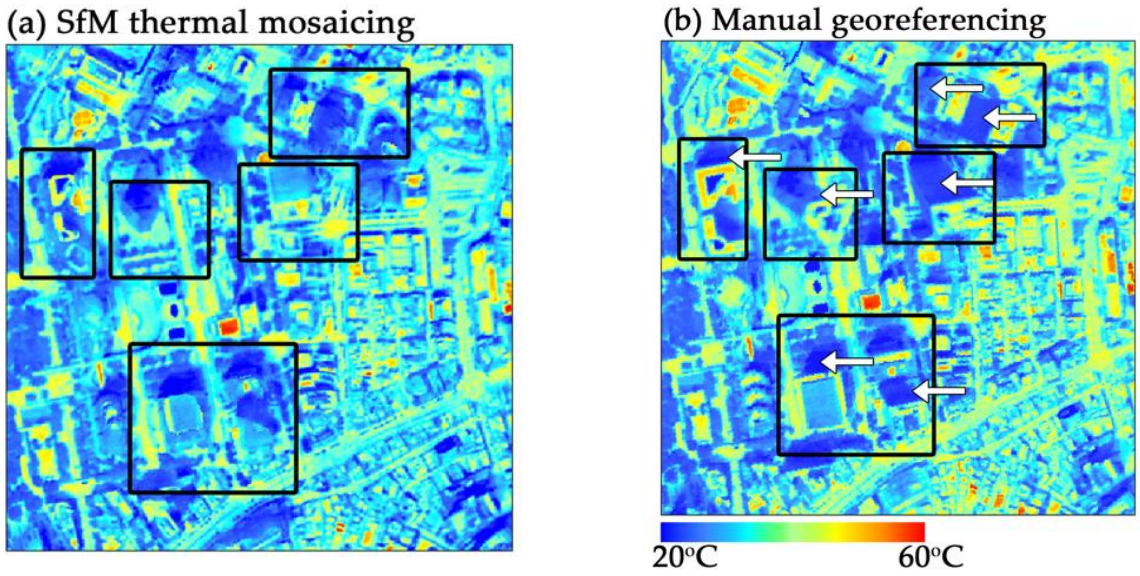

Figure 3-5: Comparison of SfM thermal mosaicing and manual georeferencing. Arrows show the side (wall) of the building.

4 CONCLUSION

Based on the error distance analysis we conclude that it is possible to make the LST image effectively with high accuracy both in daytime and night-time by SfM thermal mosaicing. The accuracy in small areas was better than the large area. The mean error distance of small area was about 2m. Considering the resolution was 2m, the error was nearly the best. SfM thermal mosaicing also have an advantage in making orthogonal LST image.

The accurate method in this study will be a powerful tool for further environmental studies on the LST. In the future, the airborne LST measurement will become more practical and economical with SfM thermal mosaicing and with the progress of UAV or drone and the development of small thermal cameras.

ACKNOWLEDGEMENTS

This work was partly supported by Research Support of LIXIL JS Foundation.

REFERENCES

Chen A., Yao XA, Sun R., Chen L., (2014), Effect of urban green patterns on surface urban cool islands and its seasonal variations. Urban Forestry and Urban Greening, 13(4), 646–654. doi.org/10.1016/j.ufug.2014.07.006

Chesley JT, Leier AL, White S., Torres R., (2017), Using unmanned aerial vehicles and structure-from-motion photogrammetry to characterize sedimentary outcrops: An example fromthe Morrison Formation, Utah, USA. Sedimentary Geology, 354, 1–8. doi.org/10.1016/j.sedgeo.2017.03.013

Colomina I., Molina P., (2014), ISPRS Journal of Photogrammetry and Remote Sensing Unmanned aerial systems for photogrammetry and remote sensing : A review. ISPRS Journal of Photogrammetry and Remote Sensing, 92, 79–97. doi.org/10.1016/j.isprsjprs.2014.02.013

Connors JP, Galletti CS, Chow WTL, (2013), Landscape configuration and urban heat island effects: Assessing the relationship between landscape characteristics and land surface temperature in Phoenix, Arizona. Landscape Ecology, 28(2), 271–283. doi.org/10.1007/s10980-012-9833-1

Dandois JP, Ellis EC, (2013), Remote Sensing of Environment High spatial resolution three-dimensional mapping of vegetation spectral dynamics using computer vision. Remote Sensing of Environment, 136, 259–276. doi.org/10.1016/j.rse.2013.04.005

Darlington T., Odindi J., Dube T., Nyasha T., (2017), Remote Sensing Applications : Society and Environment Remote sensing applications in monitoring urban growth impacts on in-and- out door thermal conditions : A review. Remote Sensing Applications: Society and Environment, 8(August), 83–93. doi.org/10.1016/j.rsase.2017.08.001

Dousset B., Gourmelon F., (2003), Satellite multi-sensor data analysis of urban surface temperatures and landcover. ISPRS Journal of Photogrammetry and Remote Sensing, 58(1–2), 43–54. doi.org/10.1016/S0924-2716(03)00016-9

Estoque RC, Murayama Y., Myint SW, (2017), Effects of landscape composition and pattern on land surface temperature: An urban heat island study in the megacities of Southeast Asia. Science of the Total Environment, 577, 349–359. doi.org/10.1016/j.scitotenv.2016.10.195

Honjo T., Tsunematsu N., Yokoyama H., (2017), Urban Climate Analysis of urban surface temperature change using structure-from-motion thermal mosaicing. Urban Climate. doi.org/10.1016/j.uclim.2017.04.004

James MR, Robson S., Oleire-oltmanns S., Niethammer U., (2017), Geomorphology Optimising UAV topographic surveys processed with structure-from-motion : Ground control quality, quantity and bundle adjustment. Geomorphology, 280, 51–66. doi.org/10.1016/j.geomorph.2016.11.021

Meesuk V., Vojinovic Z., Mynett AE, Abdullah AF, (2015), Urban flood modelling combining top-view LiDAR data with ground-view SfM observations. Advances

in Water Resources, 75, 105–117. doi.org/10.1016/j.advwatres.2014.11.008

Siebert S., Teizer J., (2014), Mobile 3D mapping for surveying earthwork projects using an Unmanned Aerial Vehicle (UAV) system. Automation in Construction, 41, 1–14. doi.org/10.1016/j.autcon.2014.01.004

Streutker DR, (2002), A remote sensing study of the urban heat island of Houston, Texas. International Journal of Remote Sensing, 23 (March 2015), 2595–2608. doi.org/10.1080/01431160110115023

Weng Q., Lu D., Schubring J., (2004), Estimation of land surface temperature-vegetation abundance relationship for urban heat island studies. Remote Sensing of Environment, 89(4), 467–483. doi.org/10.1016/j.rse.2003.11.005

Westoby MJ, Brasington J., Glasser NF, Hambrey MJ, Reynolds JM, (2012), Geomorphology " Structure-from-Motion " photogrammetry : A low-cost , effective tool for geoscience applications. Geomorphology, 179, 300–314. doi.org/10.1016/j.geomorph.2012.08.021